Panfungi

ARTICLE

Open Access

https://doi.org/10.48130/panfungi-0025-0002

Panfungi **2026**, 1: e004

Transcriptome analysis at different times reveals candidate genes of triterpenoid biosynthesis in *Inonotus obliquus* under rice medium

Yingce Duan[1], Jing Wu[2], Hirokazu Kawagishi[3*] and Chengwei Liu[1*]

[1] *Key Laboratory of National Forestry and Grassland Administration on Chinese Herbal Medicine, College of Life Science, Northeast Forestry University, Harbin 150040, China*
[2] *Faculty of Agriculture, Iwate University, Morioka 020-8550, Japan*
[3] *Faculty of Agriculture, Shizuoka University, Shizuoka 422-8529, Japan*
* Correspondence: kawagishi.hirokazu@shizuoka.ac.jp (Kawagishi H); liuchw@nefu.edu.cn (Liu C)

Abstract

Triterpenoids constitute major bioactive components in *Inonotus obliquus*. Among them, inotodiol stands out for its diverse biological activities, most notably its antitumor effects, which highlight its significant potential for cancer treatment. However, its biosynthetic pathway remains unclear. In this study, a rice-based medium solid-state fermentation strategy was employed to cultivate *I. obliquus* and obtain inotodiol, ergosterol, and lanosterol with yields of 7.33, 14.61, and 108.65 mg/kg, respectively. To investigate the genes involved in triterpenoid biosynthesis, transcriptomic analysis was conducted on mycelia collected at different cultivation time points (5 and 10 d). The expression levels of triterpenoid-related genes exhibited an increasing trend, which was further validated by qPCR. Furthermore, comparative genomic analysis of triterpene modified genes identified potential modifying enzymes, including cytochrome P450s, short-chain dehydrogenases, and ergosterol biosynthesis-related genes. These findings provide crucial insights into triterpenoid biosynthesis in *I. obliquus*, and offer valuable candidate genes for further investigation of its biosynthetic pathways.

Keywords: *Inonotus obliquus*, Triterpenoid, Inotodiol, Transcriptomic analysis, Biosynthesis

Introduction

Inonotus obliquus is a medicinal macrofungus that parasitizes birch trees and forms characteristic black sclerotia[1]. It grows in high-latitude regions and is found in Russia, Finland, Norway, and northeastern China. The triterpenoid compounds present in *I. obliquus* exhibit significant pharmacological properties[2]. Currently, the most reported compounds in *I. obliquus* are tetracyclic triterpenoids derived from the lanosterol skeleton, such as inotodiol, trametenolic acid, and lanosterol[3–5]. Sagayama et al. found that these compounds have a pro-growth effect on human hair follicle dermal papilla cells, similar to that of minoxidil, a hair growth agent[6]. Inotodiol also exhibits anti-inflammatory, anticancer, and antioxidant activities[7–9]. Additionally, there are triterpenoid compounds formed through multiple oxidations of lanosterol, such as ergosterol and ergosterol peroxide. Ma et al. reported that ergosterol exhibited superior potency against prostate cancer cells (IC_{50} = 9.82 μM), while ergosterol peroxide also showed considerable cytotoxicity (IC_{50} = 38.19 μM)[10]. Therefore, studying the biosynthesis of triterpenoids derived from the lanosterol skeleton in *I. obliquus* is of significant importance.

Given that the sclerotium of *I. obliquus* has a relatively long growth cycle, and excessive harvesting may harm the ecological environment, the study focused on the mycelium as the primary research subject. The main objectives were to enhance the triterpenoid content in *I. obliquus* and investigate its triterpenoid biosynthesis pathway. Xu et al. demonstrated that methyl jasmonate and fatty acids, acting as an elicitor and stimulating additives respectively, effectively enhanced triterpenoid yield in *I. obliquus* shake flask cultures[11]. Yang et al. demonstrated that ultrasonic treatment is a promising strategy for boosting triterpenoid accumulation in *I. obliquus* mycelia[12]. Lin et al. reported that ethanol extracts from *Rhizobium indigoferae* served as an effective elicitor to promote triterpenoid accumulation in *I. obliquus* mycelia, yielding 48.2 mg/g—a fourfold increase over the untreated control (9.5 mg/g)[13]. Fradj et al. identified 18 transcripts related to terpenoid biosynthesis and showed that white birch bark has a greater impact on the transcriptome than culture with betulin[14]. Through transcriptome analysis of *I. obliquus* in seed vs fermentation cultures, Hao et al. uncovered 157 differentially expressed genes implicated in amino acids, antioxidants, and secondary metabolite processes[15]. However, the above studies have not truly explored the specific pathways of triterpenoids, the biosynthetic pathways of triterpenoids such as inotodiol in *I. obliquus* remain unclear.

In our previous study, we reported the *I. obliquus* genome sequence, which was assembled into a 38.18 Mb draft using Illumina NovaSeq and Oxford Nanopore PromethION platforms, annotated with 12,525 protein-coding genes, 81.83% of which had detectable homologs in public databases[16]. In the study, we isolated inotodiol from the mycelium of *I. obliquus* using solid-state fermentation with rice as nutrient medium, and examined the content of various triterpenoid skeletons at different times. To elucidate the biosynthesis of triterpenoids (inotodiol, lanosterol, ergosterol) in *I. obliquus*, we performed time-series RNA sequencing to identify key candidate genes. Finally, we validated our findings using quantitative PCR (qPCR). Thus, our findings advance the understanding of triterpenoid biosynthesis in *I. obliquus*.

Dates Received 24 November 2025; Revised 7 December 2025; Accepted 8 December 2025; Published online 2 February 2026

Citation: Duan Y, Wu J, Kawagishi H, Liu C. 2026. Transcriptome analysis at different times reveals candidate genes of triterpenoid biosynthesis in *Inonotus obliquus* under rice medium. *Panfungi* 1: e004 https://doi.org/10.48130/panfungi-0025-0002

© The Author(s)

Materials and methods

Strain and medium

I. obliquus strain CT5, obtained by our laboratory[16], was cultivated in potato dextrose agar for mycelial growth. Standard substance lanosterol (CAS No. 79-63-0), and ergosterol (CAS No. 57-87-4) was purchased from Shanghai Yuanye Bio-Technology (Shanghai, China).

Detection of triterpenoid skeleton compounds

Ergosterol and inotodiol (purified in the study) were analyzed using an Agilent 1260 Infinity II high-performance liquid chromatography (HPLC) system, which was equipped with a C18 chromatographic column (250 mm × 4.6 mm). The separation was achieved via a gradient elution protocol, with the operating parameters set as follows: mobile phase A consisted of acetonitrile, while mobile phase B was ultrapure water; the ultraviolet (UV) detection wavelength was fixed at 210 nm; the column temperature was maintained at 30 °C; and the mobile phase flow rate was set to 1.0 mL/min. The specific gradient elution program was designed as follows: 90%–95% mobile phase A (0–12 min); isocratic elution with 95% mobile phase A (12–15 min); linear gradient from 95% to 100% mobile phase A (15–16 min); and isocratic elution with 100% mobile phase A (16–39 min).

Triterpenoids were detected by GC-MS (TQ8050NX, Shimadzu, Japan), and maintained at 170 °C for 2 min. From 170 to 290 °C at 10 °C/min for 4 min; and the temperature was changed from 290 to 330 °C at 10 °C/min for 10 min, and the total duration was 32 min. The ion source temperature is 230 °C, and the interface temperature is 280 °C.

Preparation of standard curves

Lanosterol was detected by GC-MS, and the derivatization method was as follows: 200 μL dissolved ethyl acetate sample was placed in 1.5 mL, lyophilized, and centrifuged for 30 min. After solvent evaporation, 30 μL of a derivatization reagent comprising imidazol-1-yl(trimethyl)silane in pyridine (CAS: 8077-35-8) was added, and the reaction was carried out at 70 °C in a metal bath for 30 min. 200–300 mL chromatography-grade ethyl acetate was added, 0.22 μm was overcoated, and then added into a liquid phase vial. GC-MS detection was performed. The gradient concentration of lanosterol was 0.05, 0.1, 0.2, 0.5, and 1.0 mg/mL (standard curve).

Purification of inotodiol from *I. obliquus* mycelium

I. obliquus mycelia were cultured on 500 g rice medium (rice : water = 1:1.5–2) and incubated at 30 °C for 15–20 d. The mature mycelial cultures were brown, and subjected to extraction with ethyl acetate. Crude extract residue was concentrated via reduced-pressure evaporation to obtain. This crude product was further fractionated through silica gel column (200–300 mesh), with an elution gradient of hexane-ethyl acetate (volume ratios ranging from 20:1 to 9:1) applied in a stepwise manner. Target fractions enriched with the target component were subsequently purified by HPLC to achieve the isolation of the desired compound. The structure of the isolated inotodiol was elucidated by nuclear magnetic resonance (NMR) spectroscopy on a Bruker AVANCE III HD 500 spectrometer. Chemical shifts (δ) are reported in parts per million (ppm), and were calibrated using $CDCl_3$ as the internal standard (^{1}H NMR: δ7.26 ppm; ^{13}C NMR: δ77.16 ppm). The molecular weight of inotodiol was confirmed by liquid chromatography-mass spectrometry (LC-MS) analysis on a Shimadzu LC-MS-9030 system. The separation was performed using a mobile phase consisting of 0.1% formic acid in water (A), and acetonitrile (B) at a flow rate of 0.3 mL/min. The gradient program was as follows: 0–1 min, 20% B; 1–13 min, 20%–100% B; 13–15 min, 100% B; 15–16 min, 100%–20% B.

RNA-seq library construction and sequencing

Transcriptome sequencing and analysis of *I. obliquus* mycelia cultured on rice medium for 5 and 10 d were performed. Total RNA was extracted from mycelia collected at each time point and reverse-transcribed into cDNA. Sequencing libraries were constructed by Biomarker Technologies Co., Ltd, and subjected to high-throughput sequencing on an Illumina platform. Raw sequencing data were processed to remove adapter sequences and low-quality reads. Clean reads were then aligned to the reference genome using HISAT2 software[17] to determine their genomic locations. Transcript assembly and splicing analysis were performed using Cufflinks. Subsequently, gene expression levels were quantified, and differentially expressed genes (DEGs) were identified based on the expression profiles between the two time points.

Differential expression analysis and functional annotation of DEGs

DEGs were identified based on gene count values from each sample using established statistical software. For comparisons with biological replicates, DESeq2[18] was applied, while edgeR[19] was used for comparisons lacking replicates. DEGs were screened using the following thresholds: $|\log_2 \text{fold change}| \geq 1$ and false discovery rate (FDR) < 0.01. The fold change reflects the ratio of expression levels between two sample groups, and the FDR represents the adjusted *p*-value that accounts for multiple testing. For comparative purposes, fold change values were $\log_2$-transformed (denoted as $\log_2$FC). A larger absolute $\log_2$FC value combined with a smaller FDR value indicates a more statistically significant difference in gene expression between groups.

Differential expression analysis was performed by comparing gene expression levels across sample groups. DEGs were functionally annotated using three databases: Cluster of Orthologous Groups (COG), Gene Ontology (GO), and Kyoto Encyclopedia of Genes and Genomes (KEGG). The COG database, built upon phylogenetic relationships across bacteria, algae, and eukaryotes, classifies gene products into orthologous categories. This classification reflects the distribution of genes across functional groups and helps reveal metabolic or physiological biases in the dataset. The GO database organizes functional knowledge into three domains: biological process, molecular function, and cellular component. Based on annotation results, DEGs were categorized and statistically analyzed at the secondary GO level to identify predominant functional attributes associated with the gene set. The KEGG database enables systematic analysis of gene functions and genomic information within integrated molecular networks. It offers comprehensive metabolic pathway mapping—including carbohydrate, nucleotide, and amino acid metabolism, as well as biodegradation processes—serving as a key resource for metabolic analysis and network-based investigations in biological systems.

Quantitative PCR (qPCR) analysis

Mycelial samples of *I. obliquus* harvested at 5 and 10 d after inoculation were subjected to total RNA isolation using Vazyme RNA-easy Isolation Reagent (Catalog No. R701). The purified RNA was reverse-transcribed into complementary DNA (cDNA) with Takara Reverse Transcription Reagent (Catalog No. 6215A). Quantitative real-time

PCR (qPCR) assays were carried out following the standard protocol provided by the manufacturer of ChamQ Universal SYBR qPCR Master Mix, with β-actin employed as the housekeeping gene[20,21]. All primers in the study are detailed in Supplementary Table S1. Three technical replicates were set up for each gene in the qPCR reactions. The relative expression levels of target genes were determined via the $2^{-\Delta\Delta C_T}$ algorithm[21].

Statistical analysis and data availability

Data were analyzed with SPSS 25 (IBM, USA), and GraphPad Prism 8 (GraphPad Software, USA), and are presented as mean ± SE. An independent samples t-test was used to assess inter-group differences, with a significance level of $p < 0.05$. The reference genome was obtained from the NCBI database (No. GCA_023101745.1).

Results

Structural identification of inotodiol

Inotodiol is a unique compound found in *I. obliquus*, notable for its distinct structure, which exhibits enhanced polarity, an attribute attributable to its two hydroxyl groups, one of which is added at C-22 relative to lanosterol. However, inotodiol is usually present in low concentrations, making its extraction and isolation quite challenging. In this study, we used rice as the growth medium for solid-state fermentation, incubating it for 20 d prior to extracting the compounds with ethyl acetate. Thin-layer chromatography analysis showed a distinct spot, indicating a compound with higher polarity than lanosterol. Then, silica gel chromatography and semi-preparative HPLC were used for further purification, and 10 mg of pure inotodiol was obtained. This purified compound was dissolved in $ClCD_3$ for nuclear magnetic resonance (NMR) analysis, The results confirmed the identity of the compound as inotodiol. ^{13}C NMR (126 MHz) δ_C 135.17, 134.58, 134.20, 121.35, 78.99, 73.39, 50.40, 49.41, 47.27, 44.87, 41.69, 38.90, 37.04, 35.59, 30.97, 30.97, 29.12, 27.97, 27.85, 27.25, 26.52, 25.99, 24.31, 21.01, 19.14, 18.25, 17.99, 15.69, 15.42, 12.62.^1H NMR (500 MHz, Chloroform-d) δ_H 5.18 (t, J = 7.3 Hz, 1H), 3.67 (dt, J = 8.0, 4.0 Hz, 1H), 3.24 (dd, J = 11.6, 4.4 Hz, 1H), 1.75 (s, 3H), 0.99 (d, J = 9.0 Hz, 4H), 0.88 (d, J = 5.1 Hz, 4H), 0.81 (s, 2H), 0.73 (s, 2H), (Supplementary Figs S1, S2). It is consistent with the literature[22]. The molecular weight of high-resolution electrospray ionization mass spectrometry analysis was found to be 443.3880 according to calcd for $C_{30}H_{50}O_2$ $[M + H]^+$:443.3884 (Fig. 1).

Variations of triterpenoid compound content in *I. obliquus* at different times

Given that *I. obliquus* exhibits higher inotodiol production when cultured on the rice medium for a long time, rice-based solid culture medium was used for its cultivation. The fungus was incubated at 30 °C for 5, 10, and 15 d, respectively, followed by extraction using ethyl acetate through soaking. After vacuum distillation, the extracts were analyzed via GC-MS. Three triterpenoid compounds—lanosterol, ergosterol, and inotodiol were identified in *I. obliquus* (Fig. 2a). Following the derivatization of lanosterol, the main fragment peaks observed were 393 (100%), 483 (25%), and 498 (20%) in the GC-MS analysis. For ergosterol, the main fragment peaks were 363 (100%), 337 (75%), 253 (25%), 378 (25%), 468 (20%), and 396 (5%). In the case of inotodiol, the main peaks were 337 (100%), 297 (75%), 427 (25%), and 517 (10%) (Fig. 2b). These findings align with previously reported references[23,24]. Quantitative analysis of three triterpenoid compounds showed that their contents increased with the extension of the cultivation period (Fig. 2c). At 5 d, the concentrations of all three triterpenoids remained relatively low. Notably, the expression level of ergosterol was extremely low during the early stages of *I. obliquus* cultivation. Due to the limited biomass of *I. obliquus* mycelium at 5 d, ergosterol was undetectable by HPLC, and its concentration fell below the detection limit of GC-MS, preventing any quantification. However, by 10 d, the levels of all three triterpenoids began to increase. The rate of accumulation observed between 5 and 10 d was lower than that between 10 and 15 d. At 15 d, the concentrations of all three triterpenoids reached their highest levels: ergosterol (14.61 mg/kg), inotodiol (7.33 mg/kg), and lanosterol (> 108.65 mg/kg), indicating robust production during the mycelial stage. This abundance also provides ample precursor substances for the biosynthesis of various lanostane-type triterpenoids.

Transcriptomic sequencing analysis of *I. obliquus* at different times

During the cultivation of *I. obliquus* in the rice medium from 5 to 15 d, the levels of triterpene compounds—lanosterol, ergosterol, and inotodiol—increased over time. At 15 d, the color of the mycelium were observed to have changed from its earlier white to brown. We could not confirm whether new peak values appeared between days 10 and 15, as it is highly likely that the trend followed an initial increase followed by a decline. Transcriptomic analysis was therefore conducted on *I. obliquus* cultures from day 5 to day 10 to track the expression changes of genes involved in triterpene biosynthesis. Following quality control, the sequencing yielded 40.54 Gb of high-quality data, with all samples exhibiting a Q30 base percentage above 98.24%. Alignment of the reads to the reference genome demonstrated high efficiency, with rates ranging from 90.19% to 95.19% across the samples (Supplementary Tables S2, S3).

Analysis and functional annotation of differential genes in the transcriptome

Transcriptome profiling across different time points in *I. obliquus* revealed a total of 316 DEGs. Among these, 180 were up-regulated, and 136 were down-regulated (Fig. 3). Functional annotations of

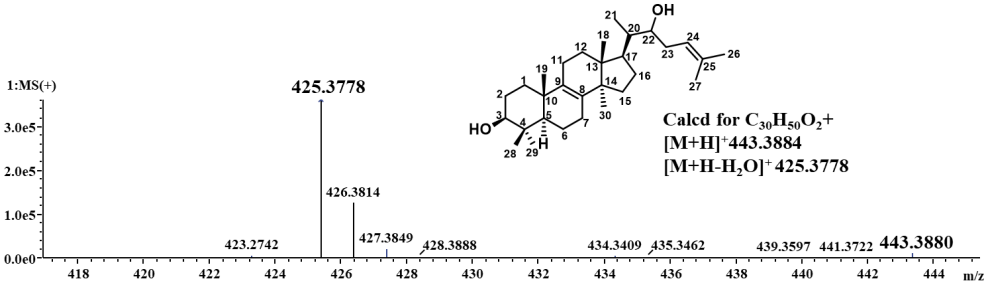

Fig. 1 Detection of inotodiol by LC-MS.

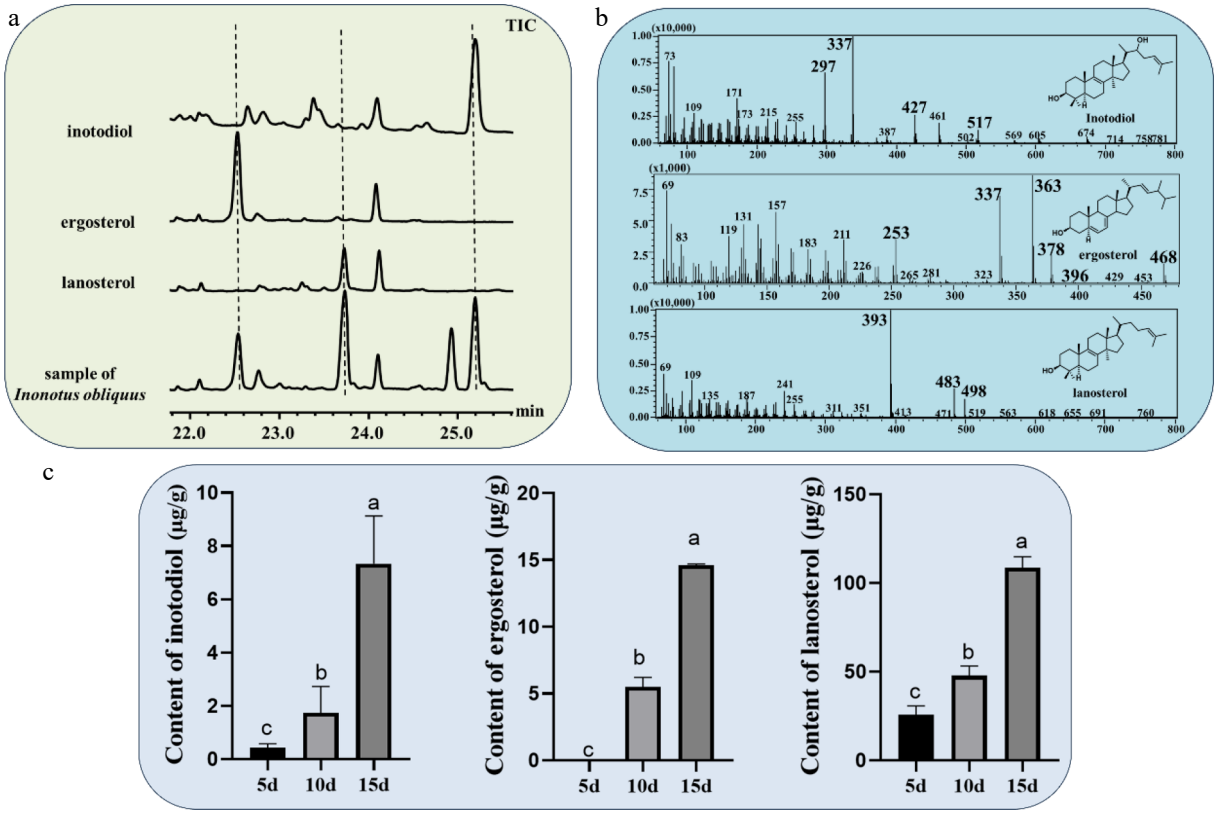

Fig. 2 (a) GC-MS chromatograms analysis sample of *I. obliquus* in rice culture medium and three triterpene skeleton standards. (b) Mass spectra of inotodiol, ergosterol, and lanosterol. (c) Content of different triterpenoids in *I. obliquus* under different times.

differentially expressed genes in CT5-5_vs_CT5-10 were conducted in various databases, with 124 in COG, 186 in GO, 158 in KEGG, 96 in KOG, 272 in NR, 179 in Pfam, and 127 in Swiss-Prot.

A total of 124 DEGs were classified and statistically analyzed by COG, and the results are shown in Fig. 4a. The differentially expressed genes of *I. obliquus* mainly distributed in five modules: G module (carbohydrate transport and metabolism), E module (amino acid transport and metabolism), Q module (secondary metabolism biosynthesis, transport and metabolism), R module (used only for general function prediction), and V module (defense mechanism). This indicates that during the growth process, the gene module for carbohydrate transport and metabolism is constantly functioning. Not only during the mycelial growth process, but also during the accumulation of secondary metabolites and participation in defense mechanisms. During the process of mycelia absorbing nutrients from the environment, they also face challenges from the environment, thus requiring the secretion of some secondary metabolites to protect themselves. GO annotation (biological processes, cellular components, and molecular functions) identified 186 DEGs. From Fig. 4b, the biological processes with the largest number of DEGs are distributed in metabolic processes and cellular processes; in terms of cellular components, they are mainly concentrated in cellular anatomical entities; and in terms of molecular functions, they are mainly catalytic activities and transport functions. During the growth process from 5 to 10 d, *I. obliquus* is more focused on mycelial growth, so the differentially expressed genes are mainly concentrated in metabolic processes and cellular processes. KEGG annotation identified 158 DEGs (Fig. 4c, d), and these genes are also mainly concentrated in the metabolic processes of amino sugars and nucleotide sugars. Up-regulated genes include glycosphingolipid biosynthesis—ganglioseries and glycine degradation; down-regulated genes include glyoxylate and dicarboxylate metabolism, and nitrogen metabolism.

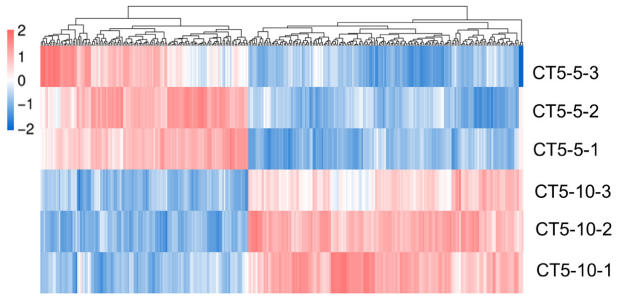

Fig. 3 Differential gene distribution of transcriptome at different times.

Analysis of key differential genes in the transcriptome

Compared to 5-d *I. obliquus* mycelia, 10-d exhibited more vigorous growth. Among the differentially expressed genes, 24 candidate genes (19 upregulated and five downregulated) were involved in carbohydrate transport and metabolism (Fig. 5a). This indirectly suggests that energy metabolism remains the dominant factor during the growth period from 5 to 10 d. To identify key genes related to triterpenoid biosynthesis, we must examine the expression patterns of genes involved in the mevalonate (MVA) pathway, which is the source pathway for terpene formation in fungi and terpene synthase-related genes. Firstly, we discovered different expression levels of related genes on the MVA pathway from acetyl-CoA to the formation of farnesyl pyrophosphate (FPP) in *I. obliquus* at different times (Supplementary Table S4). According to the transcriptome data, most genes in the MVA pathway show an upward trend with time. Among them, the expression levels of mevalonate kinase and mevalonate pyrophosphate decarboxylase decrease with

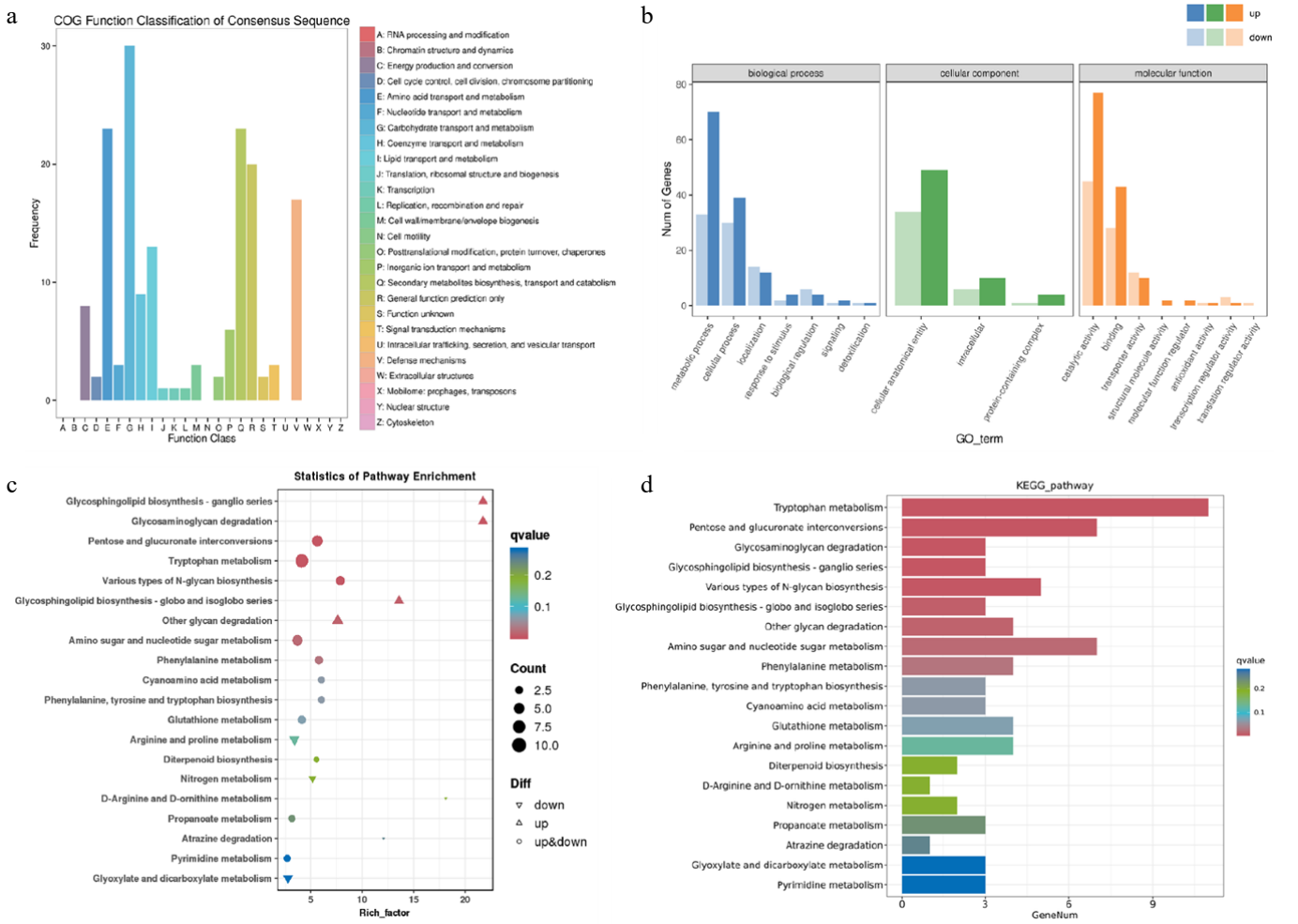

Fig. 4 Functional classification and enrichment analysis of DEGs between the 5 and 10vd groups. (a) COG functional classification of DEGs. (b) GO enrichment analysis of DEGs. (c) KEGG pathway enrichment analysis of DEGs. The rich factor represents the degree of enrichment. (d) KEGG functional classification of DEGs. The bar length indicates the number of DEGs involved in each pathway.

time. This can be attributed to the involvement of upstream pathways in more complex metabolic networks, which are subject to diverse regulatory mechanisms. The expression levels of other terpene synthase genes are mostly very low, with FPKM values generally below 10 (Supplementary Fig. S6). From the overall expression in the mycelial stage, although there are slight changes, the expression levels of many genes are extremely low, and more belong to silent genes, which are also typical secondary metabolic genes. Squalene is converted to lanosterol through the sequential catalytic actions of squalene monooxygenase (g1801), and lanosterol synthase (g2189), the latter being the sole identified triterpenoid synthase in the genome. Transcriptome analysis revealed an upward trend in the expression of these genes (Fig. 5b), which is consistent with the phenotypic data. Since fungal cell membranes are composed of sterols, lanosterol subsequently serves as a precursor for ergosterol biosynthesis. This suggests that during the observed growth phase, both triterpenoid and ergosterol biosynthesis pathways are active, with lanosterol acting as a key branching point for metabolic flux toward different sterol and triterpenoid derivatives. The biosynthetic pathway of ergosterol has been well-characterized in *Saccharomyces cerevisiae*[25,26]. The expression levels of candidate genes from the ergosterol biosynthesis are shown in Fig. 5b. Based on the changes in the yields of lanosterol and ergosterol, both compounds increased over time (5–10 d), and transcriptome data revealed that 14 genes involved in their biosynthesis showed an upward trend. The expression levels of genes are positively correlated with the yields of products. The lanosterol and ergosterol biosynthesis pathways are positively correlated with time and content. Therefore, it is speculated that the genes related to the biosynthesis of triterpenoids, such as inotodiol, are also positively correlated with time and content. Analysis of P450 gene expression in *I. obliquus* revealed 25 upregulated and 23 downregulated P450 candidate genes (Fig. 5c and Supplementary Fig. S7). The upregulated P450 genes primarily belong to gene families such as CYP5144, CYP5969, and CYP5423, suggesting their potential involvement in oxidative modifications during triterpenoid biosynthesis. Additionally, short-chain dehydrogenases (SDRs) were identified that may participate in triterpenoid biosynthesis. Based on domain analysis, 21 candidate SDR genes were detected, but their expression patterns were irregular. Most exhibited higher expression at 5 d, while their levels decreased significantly by 10 d. This temporal regulation implies that SDRs might play a more prominent role in the early stages of triterpenoid metabolism, possibly in oxidoreduction reactions (e.g., C3-carbonylation interconversion[27]) before the major biosynthetic flux shifts toward downstream modifications (Supplementary Figs S8, S9).

qPCR verification of key transcriptome genes at different times

The housekeeping gene actin (g4179) in *I. obliquus* was used as the internal reference for genes involved in ergosterol biosynthesis.

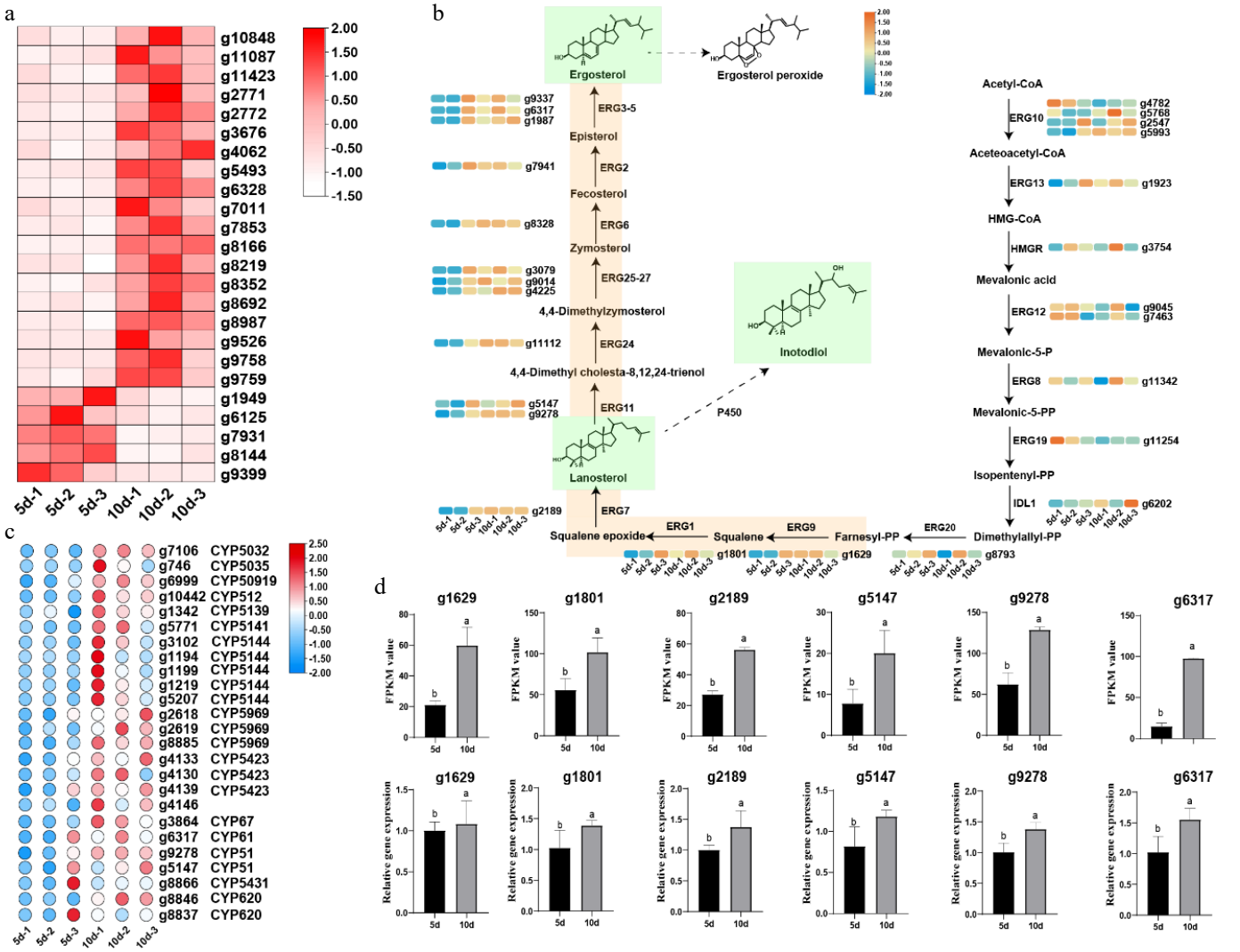

Fig. 5 Analysis and validation of key metabolic pathways during the developmental transition (5 vs 10 d). (a) Expression profiles of differentially expressed genes (DEGs) related to carbohydrate transport and metabolism. (b) DEGs involved in the mevalonate (MVA) pathway and downstream ergosterol biosynthesis. (c) Heatmap of cytochrome P450 (CYP450)-related DEGs, showing a predominant upregulation pattern. (d) Quantitative PCR (qPCR) validation of selected genes from the triterpenoid and ergosterol biosynthesis pathways at 5 and 10 d. Data are presented as mean ± SD (n = 3). The classification of the CYP family was directly distinguished based on the CYP database website (https://p450atlas.org/index.html).

Six genes from the ergosterol pathway were validated by qPCR, including upstream enzymes—lanosterol synthase (g2189), squalene synthase (g1629), and squalene epoxidase (g1801)—as well as downstream enzymes—lanosterol 14α-demethylase (g9278 and g5147), and sterol C-22 desaturase (g6317). As shown in Fig. 5d, the expression levels of lanosterol synthase, squalene synthase, squalene epoxidase, and ergosterol synthase-related genes exhibited a time-dependent increase, which aligned with the transcriptomic data trends, further confirming transcriptome analysis data.

Discussion

In this study, solid-state fermentation of *I. obliquus* mycelium was conducted on a rice medium. After the mycelium covered the rice, ethyl acetate extraction was carried out, and finally, inotodiol was isolated and identified by nuclear magnetic resonance. The study found that *I. obliquus* produced close to 10 mg of inotodiol per 1 kg of rice, though conservative estimates were reported due to insufficient calculations. Currently, most of the inotodiol and lanosterol isolation is mainly from sclerotia. Therefore, the separation and purification was carried out at the mycelial stage, providing a simple way to obtain inotodiol and lanosterol. This study utilized a rice-based culture medium to explore terpenoid compounds in mushrooms, representative example *Cordyceps militaris*[28], diterpene from *Hericium erinaceus*[29], and sesquiterpenoids of *Stereum hirsutum*[30]. While this approach is not novel, it significantly reduces the required time. The natural sclerotium formation is a prolonged process, and wild harvesting has led to depletion of *I. obliquus* resources. Through short-term rice cultivation of *I. obliquus*, followed by isolation and extraction, medically valuable inotodiol with good efficiency was successfully obtained. In the study, *I. obliquus* mycelium was grown on a rice medium, and GC-MS detection confirmed the presence of triterpenoid compounds such as inotodiol, lanosterol, and ergosterol at the mycelial stage. The three triterpenoid compounds in *I. obliquus* were detected at different times (5, 10, and 15 d), and it was found that their contents increased with time, proving that the three triterpenoids were enriched during the 5–15 d growth process. Duan et al. determined the contents of different triterpenoids (ergosterol, lanosterol, inotodiol, and trametenolic acid) as an important index to evaluate the quality of the sclerotium, providing a reference for a comprehensive

and objective evaluation of the quality of *I. obliquus*[31]. Cao et al. found that different nutritional conditions changed the triterpene content in *I. obliquus*. Samples of 5 and 10 d were also selected to determine the contents of lanosterol and inotodiol[32]. The trend verified the results of this study, both indicating a progressive increase.

In this study, 316 DEGs were identified, and the transcription levels of the MVA pathway and ergosterol biosynthesis genes were detected. The key genes in triterpenoid synthesis were verified by qPCR. The accuracy of the transcriptome was determined, and the increase in triterpene content was positively correlated with the increase in triterpene-related gene expression. With the discovery of triterpenoid biosynthesis in fungi, it has been found that some genes from the ergosterol pathway also participate in the biosynthesis of some triterpenoids in mushroom. For example, ERG6, a sterol C-24 methyltransferase in ergosterol biosynthesis, is involved in the transfer of double bonds in triterpenoids. In *Poria cocos*, PcSMT1-1 (KY704878) can convert trametenolic acid into eburicoic acid[33]. In *Antrodia cinnamomea*, AcSMT1 (PQ433312) can convert 3β,15α-dihydroxylanosta-7,9(11),24-triene-21-oic acid into dehydrosulphurenic acid[27]. In yeast, the sterol C-3 ketoreductase ERG27 can reduce the carbonyl group at the C-3 position of ganoderic acid DM in *Ganoderma* to a hydroxyl group[34]. Meanwhile, short-chain dehydrogenases also play an important role in triterpenoid biosynthesis, oxidizing the hydroxyl group at the C-3 position to a carbonyl group. In *A. cinnamomea*, AcSDR6 converts dehydroeburicoic acid into dehydroeburiconic acid[27]. In *I. obliquus*, the compounds 3-oxo-lanosta-8,24-diene-21-al and 3β,21-dihydroxy-lanosta-8,24-diene were discovered[35], suggesting that they may be formed under the action of short-chain dehydrogenases or ERG27 (Fig. 6).

P450 enzymes are pivotal drivers of structural diversification in triterpenoid biosynthesis, with different families catalyzing site-specific modifications across the triterpenoid scaffold. At present, P450 involved in the biosynthesis of many triterpenoids has been reported in *Ganoderma lucidum*. For instance, CYP505D13 can catalyze the formation of ST-3 from squalene[36]. CYP5150L8 is capable of the multi-step oxidation of lanosterol at C-26, progressing through hydroxylated (HLDO) and aldehyde (HLDA) intermediates to generate the carboxylated product (HLDOA)[37]. We hypothesize that the P450 gene modifying lanosterol might be part of the CYP5150 family in *I. obliquus* and also be involved in the biosynthesis of trametenolic acid. The compounds 3β,21-dihydroxy-lanosta-8,24-diene (hydroxylation), 3β-hydroxy-lanosta-8,24-dien-21-al (aldehydation), and trametenolic acid (carboxylation) are sequentially oxidized derivatives of lanosterol at the C-21 position, all of which have been isolated from Chaga mushroom[38]. This process is extremely similar to the mechanism of action of CYP5150L8 (C-26 position modification) (Fig. 6). CYP5139G1 in *G. lucidum* undergoes oxidation at the C-28 site using HLDOA as the substrate to form DHLDOA[39]. CYP512 family reported in fungi mainly uses intermediate triterpenoids as the skeleton for remodification. CYP512U6 in *G. lucidum* catalyzes the C-23 hydroxylation of ganoderic acids DM and

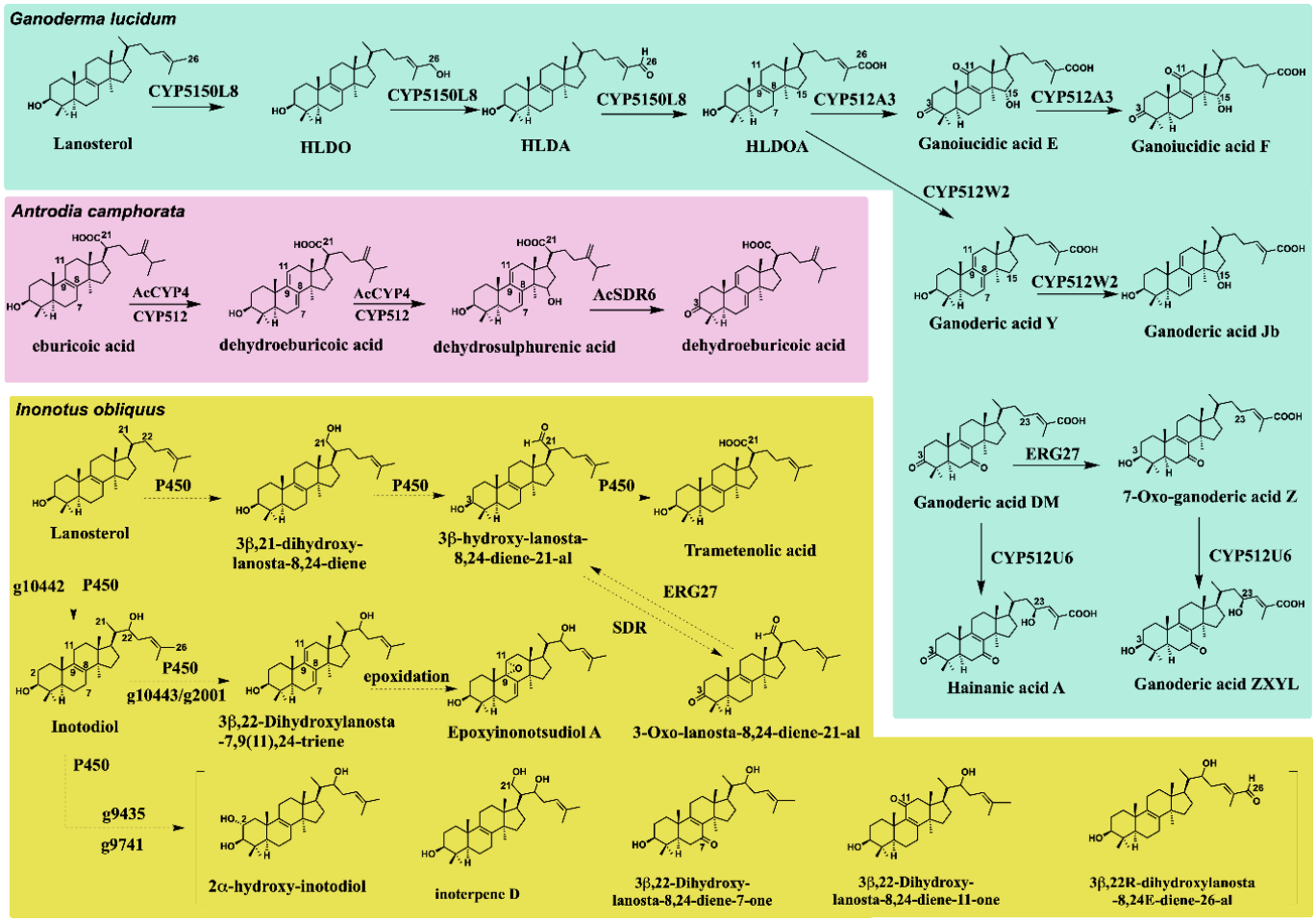

Fig. 6 Based on the functional analysis of P450, SDR, and ERG27 in *G. lucidum* and *A. camphorata*, the biosynthetic pathway of reported triterpenoids in *I. obliquus* was speculated. Solid lines indicate experimentally confirmed reaction conversions; dashed lines to represent predicted reactions in the study.

TR[34]. CYP512A3 catalyzes carbonylation at C-3 and C-11 positions in HLDOA, and can also catalyze hydroxylation at C-15 position[40]. The CYP512 family can catalyze the positional shift of double bonds in triterpenes, converting the Δ8 double bond into a Δ7,9(11) diene structure. AcCYPA4 in *A. camphorata* can catalyse the formation of eburicoic acid from dehydroeburicoic acid, and further catalyse the formation of dehydrosulphurenic acid[27]. CYP512W2 and CYP512A2 in *G. lucidum* are modified to form type II ganoderic acid using HLDOA as the skeleton[41]. Therefore, it is hypothesized that the CYP512 family of *I. obliquus* may catalyze the conversion of inotodiol into 3β,22-dihydroxylanosta-7,9(11),24-triene (reported in Chaga mushroom[42]). The epoxidation of this compound forms epoxyinonotsudiol A (epoxy ring formed between C-9 and C-11)[43]. Many triterpene compounds from *I. obliquus* might be derived from compounds with inotodiol as the framework, such as 2α-hydroxy-inotodiol (hydroxylation at the C-2 position)[44], 3β,22-dihydroxy-lanosta-8,24-diene-7-one (carbonylation at the C-7 position)[45], 3β,22-dihydroxy-lanosta-8,24-diene-11-one (carbonylation at the C-11 position)[46], inoterpene D (hydroxylation at the C-21 position)[47], 3β,22*R*-dihydroxylanosta-8,24E-diene-26-al (aldehydation at position C-26)[48] (Fig. 6). Moreover, many of these biochemical reactions involved inotodiol and lanosterol are very likely catalyzed by P450 enzymes, so transcriptomic data analysis in *I. obliquus* was performed to examine the screened candidate P450 which may contain genes related to the biosynthesis of triterpenoids (Fig. 5c and Supplementary Fig. S10). The differentially expressed genes identified through transcriptome screening in this study provide candidate genes for triterpenoid biosynthesis, opening new perspectives for further research on triterpenoid biosynthesis. In the future, functional characterization of these candidate genes can be carried out using approaches such as isotope labeling, heterologous expression, or gene knockout/knockdown. These experimental strategies will help validate the roles of the candidate genes and further elucidate and refine the triterpenoid biosynthetic pathway in *Inonotus obliquus*.

Conclusions

In this study, inotodiol was isolated from *I. obliquus* mycelia cultured on rice medium and identified using NMR and LC-MS. Subsequently, it was observed that the contents of three triterpenoids (ergosterol, inotodiol, and lanosterol) in *I. obliquus* increased over time when grown on rice medium. Comparative transcriptome analysis of *I. obliquus* mycelia (5 vs 10 d) identified 316 DEGs. Further analysis focused on the MVA pathway and ergosterol biosynthesis pathway in *I. obliquus*, followed by qPCR validation of key DEGs. This led to the identification of P450s and SDRs potentially involved in triterpenoid biosynthesis and modification. These findings pave the way for the systematic elucidation of triterpenoid biosynthetic mechanisms in *I. obliquus*.

Ethical statements

Not applicable.

Author contributions

The authors confirm their contributions to the paper as follows: conceptualization: Liu CW, Duan YC; methods, software, experiment and data organization: Duan YC, Wu J; writing original draft: Duan YC; review and editing: Kawagishi H, Liu CW; funding acquisition: Liu CW. All authors reviewed the results and approved the final version of the manuscript.

Data availability

The raw sequencing data supporting the findings of this study can be accessed in the NCBI Sequence Read Archive (SRA) under the BioProject accession PRJNA1253771.

Acknowledgments

We gratefully acknowledge Dr. Dan Sui from the Instrumental Analysis Center at Northeast Forestry University for her assistance with NMR analysis. This work was supported by the Fundamental Research Funds for the Central Universities (No. 2572023AW40), the National Natural Science Foundation of China (Nos 32370069 and U22A20369), and the Natural Science Foundation of Heilongjiang Province of China (No. LH2023C035).

Conflict of interest

The authors declare no competing interests.

Supplementary information accompanies this paper online at (https://doi.org/10.48130/panfungi-0025-0002)

References

[1] Lee MW, Hur H, Chang KC, Lee TS, Ka KH, et al. 2008. Introduction to distribution and ecology of sterile conks of *Inonotus obliquus*. *Mycobiology* 36:199–202

[2] Plehn S, Wagle S, Rupasinghe HPV. 2023. Chaga mushroom triterpenoids as adjuncts to minimally invasive cancer therapies: a review. *Current Research in Toxicology* 5:100137

[3] Zheng W, Miao K, Liu Y, Zhao Y, Zhang M, et al. 2010. Chemical diversity of biologically active metabolites in the sclerotia of *Inonotus obliquus* and submerged culture strategies for up-regulating their production. *Applied Microbiology and Biotechnology* 87:12371254

[4] Ern PTY, Quan TY, Yee FS, Yin ACY. 2024. Therapeutic properties of *Inonotus obliquus* (Chaga mushroom): A review. *Mycology* 15:144–161

[5] Duan Y, Sui D, Wang L, Zhang X, Wang C, Liu C. 2022. Research progress on small molecule chemical components and pharmacological values of *Inonotus obliquus*. *Journal of Fungal Research* 20(3):214–227 (in Chinese)

[6] Sagayama K, Tanaka N, Fukumoto T, Kashiwada Y. 2019. Lanostane-type triterpenes from the sclerotium of *Inonotus obliquus* (Chaga mushrooms) as proproliferative agents on human follicle dermal papilla cells. *Journal of Natural Medicines* 73:597–601

[7] Zhang X, Bao C, Zhang J. 2018. Inotodiol suppresses proliferation of breast cancer in rat model of type 2 diabetes mellitus via downregulation of β-catenin signaling. *Biomedicine & Pharmacotherapy* 99:142–150

[8] Chung J, Choi MR, Park S, Kang JY, Chung EH, et al. 2023. Inotodiol suppresses allergic inflammation in allergic rhinitis mice. *International Forum of Allergy & Rhinology* 13:1603–1614

[9] Lee SH, Won GW, Choi SH, Kim MY, Oh CH, et al. 2022. Antiaging effect of inotodiol on oxidative stress in human dermal fibroblasts. *Biomedicine & Pharmacotherapy* 153:113311

[10] Ma L, Chen H, Dong P, Lu X. 2013. Anti-inflammatory and anticancer activities of extracts and compounds from the mushroom *Inonotus obliquus*. *Food Chemistry* 139:503–508

[11] Xu X, Zhang X, Chen C. 2016. Stimulated production of triterpenoids of *Inonotus obliquus* using methyl jasmonate and fatty acids. *Industrial Crops and Products* 85:49–57

[12] Wang Y, Liu X, Sun L, Dou B, Xin J, et al. 2024. Physical radiation induced the yield of triterpenoids in hypha of *Inonotus obliquus* to increase. *Journal of Microbiological Methods* 225:107025

[13] Lin P, Yan ZF, Li CT. 2020. Effects of exogenous elicitors on triterpenoids accumulation and expression of farnesyl diphosphate

synthase gene in *Inonotus obliquus*. *Biotechnology and Bioprocess Engineering* 25:580−588

[14] Fradj N, Gonçalves Dos Santos KC, de Montigny N, Awwad F, Boumghar Y, et al. 2019. RNA-Seq de novo assembly and differential transcriptome analysis of chaga (*Inonotus obliquus*) cultured with different betulin sources and the regulation of genes involved in terpenoid biosynthesis. *International Journal of Molecular Sciences* 20(18):4334

[15] Hao J, Wang X, Shi Y, Li L, Chu J, et al. 2023. Integrated omic profiling of the medicinal mushroom *Inonotus obliquus* under submerged conditions. *BMC genomics* 24:554

[16] Duan Y, Han H, Qi J, Gao JM, Xu Z, et al. 2022. Genome sequencing of *Inonotus obliquus* reveals insights into candidate genes involved in secondary metabolite biosynthesis. *BMC genomics* 23:314

[17] Kim D, Paggi JM, Park C, Bennett C, Salzberg SL. 2019. Graph-based genome alignment and genotyping with HISAT2 and HISAT-genotype. *Nature Biotechnology* 37:907−915

[18] Love MI, Huber W, Anders S. 2014. Moderated estimation of fold change and dispersion for RNA-seq data with DESeq2. *Genome Biology* 15:550

[19] Robinson MD, McCarthy DJ, Smyth GK. 2010. edgeR: a Bioconductor package for differential expression analysis of digital gene expression data. *Bioinformatics* 26:139−140

[20] Li L, Guo X, Wang S. 2025. Selection and evaluation of reference genes for qRT-PCR in *Inonotus obliquus*. *Frontiers in Microbiology* 16:1500043

[21] Hou L, Wang L, Wu X, Gao W, Zhang J, et al. 2019. Expression patterns of two pal genes of *Pleurotus ostreatus* across developmental stages and under heat stress. *BMC Microbiology* 19:231

[22] Kim JH, Gao D, Cho CW, Hwang I, Kim HM, et al. 2021. A novel bioanalytical method for determination of inotodiol isolated from *Inonotus obliquus* and its application to pharmacokinetic study. *Plants* 10(8):1631

[23] Huynh N, Beltrame G, Tarvainen M, Suomela JP, Yang B. 2022. Supercritical CO_2 extraction of triterpenoids from chaga sterile conk of *Inonotus obliquus*. *Molecules* 27:1880

[24] Borrull A, López-Martínez G, Poblet M, Cordero-Otero R, Rozès N. 2015. A simple method for the separation and quantification of neutral lipid species using GC-MS. *European Journal of Lipid Science and Technology* 117:274−280

[25] Xu S, Chen C, Li Y. 2020. Engineering of phytosterol-producing yeast platforms for functional reconstitution of downstream biosynthetic pathways. *ACS Synthetic Biology* 9:3157−3170

[26] Ma BX, Ke X, Tang XL, Zheng RC, Zheng YG. 2018. Rate-limiting steps in the *Saccharomyces cerevisiae* ergosterol pathway: towards improved ergosta-5, 7-dien-3β-ol accumulation by metabolic engineering. *World Journal of Microbiology and Biotechnology* 34:55

[27] Zhang Y, Zhang M, Wang Z, Bao YO, Wang Y, et al. 2025. Identification of key post-modification enzymes involved in the biosynthesis of lanostane-type triterpenoids in the medicinal mushroom *Antrodia camphorata*. *Angewandte Chemie International Edition* 64:e202420104

[28] Wu CY, Liang CH, Liang ZC. 2022. Enhanced production of fruiting bodies and bioactive compounds of *Cordyceps militaris* with grain substrates and cultivation patterns. *Journal of the Taiwan Institute of Chemical Engineers* 132:104138

[29] Yuan L, Liu JK. 2025. Hericinosides A-M, Cyathane diterpene glycosides with α-glucosidase inhibitory activity from the medicinal fungus *Hericium erinaceus*. *Journal of Agricultural and Food Chemistry* 73:1389−1402

[30] Ma K, Bao L, Han J, Jin T, Yang X, et al. 2014. New benzoate derivatives and hirsutane type sesquiterpenoids with antimicrobial activity and cytotoxicity from the solid-state fermented rice by the medicinal mushroom *Stereum hirsutum*. *Food Chemistry* 143:239−245

[31] Duan Y, Zhu T, Chen S, Duan X, Wang S. 2023. Determination of four components of *Inonotus obliquus* by HPLC and comparison of contents in different parts. *Herald of Medicine* 42:339−345 (in Chinese)

[32] Zeng L, Liu Q, Wu H, Yang M, Cao X. 2025. Effects of nutrient restriction on growth and triterpene synthesis of *Inonotus obliquus*. *Acta Microbiologica Sinica* 65:362−370 (in Chinese)

[33] Guo J. 2017. Cloning and characterization of sterol C24 methyltransferase (SMT1) gene from *Poria cocos*. Master's Thesis. Huazhong Agricultural University, Wuhan, China

[34] Yang C, Li W, Li C, Zhou Z, Xiao Y, et al. 2018. Metabolism of ganoderic acids by a *Ganoderma lucidum* cytochrome P450 and the 3-keto sterol reductase ERG27 from yeast. *Phytochemistry* 155:83−92

[35] Zhang S, Xie Y, Tan Y, Chen H, Mei R, et al. 2015. Triterpenoids of *Inonotus obliquus*. *Chinese Traditional and Herbal Drugs* 46:2355−2360 (in Chinese)

[36] Fang Y, Luo M, Song X, Shen Y, Xiao H. 2020. Improving the production of squalene-type triterpenoid 2,3;22,23-squalene dioxide by optimizing the expression of CYP505D13 in *Saccharomyces cerevisiae*. *Journal of Bioscience and Bioengineering* 130:265−271

[37] Lan X, Yuan W, Wang M, Xiao H. 2019. Efficient biosynthesis of antitumor ganoderic acid HLDOA using a dual tunable system for optimizing the expression of CYP5150L8 and a *Ganoderma* P450 reductase. *Biotechnology and Bioengineering* 116:3301−3311

[38] Kahlos K, Tikka VH. 1994. Antifungal activity of cysteine, its effect on C-21 oxygenated lanosterol derivatives and other lipids in *Inonotus obliquus*, in vitro. *Applied Microbiology and Biotechnology* 42:385−390

[39] Wang WF, Xiao H, Zhong JJ. 2022. Biosynthesis of a novel ganoderic acid by expressing CYP genes from *Ganoderma lucidum* in *Saccharomyces cerevisiae*. *Applied Microbiology and Biotechnology* 106:523−534

[40] Du Y, Peng S, Chen H, Li J, Huang F, et al. 2025. Unveiling the spatiotemporal landscape of *Ganoderma lingzhi*: Insights into ganoderic acid distribution and biosynthesis. *Engineering*

[41] Yuan W, Jiang C, Wang Q, Fang Y, Wang J, et al. 2022. Biosynthesis of mushroom-derived type II ganoderic acids by engineered yeast. *Nature Communications* 13:7740

[42] Kahlos K, Hiltunen R. 1986. 3*β*,22-Dihydroxylanosta-7,9(11),24-triene: a new, minor compound from *Inonotus obliquus*. *Planta Medica* 00:495−496

[43] Handa N, Yamada T, Tanaka R. 2012. Four new lanostane-type triterpenoids from *Inonotus obliquus*. *Phytochemistry Letters* 5:480−485

[44] Kou RW, Xia B, Han R, Li ZQ, Yang JR, et al. 2022. Neuroprotective effects of a new triterpenoid from edible mushroom on oxidative stress and apoptosis through the BDNF/TrkB/ERK/CREB and Nrf2 signaling pathway in vitro and in vivo. *Food & Function* 13:12121−12134

[45] Kahlos K. 1986. 3β,22-Dihydroxy-lanosta-8,24-dien-7-one, a new 7-keto compound from *Inonotus obliquus*. *Acta Pharmaceutica Fennica* 95:113−117

[46] Handa N, Yamada T, Tanaka R. 2010. An unusual lanostane-type triterpenoid, spiroinonotsuoxodiol, and other triterpenoids from *Inonotus obliquus*. *Phytochemistry* 71:1774−1779

[47] Nakamura S, Iwami J, Matsuda H, Mizuno S, Yoshikawa M. 2009. Absolute stereostructures of inoterpenes A–F from sclerotia of *Inonotus obliquus*. *Tetrahedron* 65:2443−2450

[48] Chen SD, Yong TQ, Xiao C, Gao X, Xie YZ, et al. 2021. Inhibitory effect of triterpenoids from the mushroom *Inonotus obliquus* against α-glucosidase and their interaction: Inhibition kinetics and molecular stimulations. *Bioorganic Chemistry* 115:105276

Copyright: © 2026 by the author(s). Published by Maximum Academic Press on behalf of Jilin Agricultural University. This article is an open access article distributed under Creative Commons Attribution License (CC BY 4.0), visit https://creativecommons.org/licenses/by/4.0/.